The Ability of SD-OCT to Differentiate Early Glaucoma With High Myopia From Highly Myopic Controls and Nonhighly Myopic Controls

Azusa Akashi, Akiyasu Kanamori, Kaori Ueda, Yukako Inoue, Yuko Yamada, and Makoto Nakamura

Division of Ophthalmology, Department of Surgery, Kobe University Graduate School of Medicine, Kobe, Japan

Correspondence: Akiyasu Kanamori, Division of Ophthalmology, Department of Surgery, Kobe University Graduate School of Medicine, Kobe, Japan;
kanaaki@med.kobe-u.ac.jp.

Submitted: July 8, 2015
Accepted: September 9, 2015

Citation: Akashi A, Kanamori A, Ueda K, Inoue Y, Yamada Y, Nakamura M. The ability of SD-OCT to differentiate early glaucoma with high myopia from highly myopic controls and nonhighly myopic controls. *Invest Ophthalmol Vis Sci*. 2015;56:6573–6580.
DOI:10.1167/iovs.15-17635

Purpose. Optical coherence tomography (OCT) instruments do not embed a normative database from highly myopic normal (HMN) eyes. The abilities of three OCT instruments to detect early glaucoma with high myopia were compared using the two controls with or without high myopia.

Methods. A total of 52 early glaucomatous eyes (mean deviation > -6.0 dB) with high myopia (spherical equivalent ≤ -6.0 diopters [HMG]), 54 HMN eyes, and 90 nonhighly myopic normal (NHMN) eyes were enrolled. Each participant was imaged using Cirrus, RTVue, and Topcon 3D OCT to evaluate the thicknesses of the circumpapillary retinal nerve fiber layer (cpRNFL), the macular retinal nerve fiber layer (mRNFL), ganglion cell layer + inner plexiform layer (GCL/IPL), and mRNFL + GCL/IPL (GCC). The covariate-adjusted areas under the receiver operating characteristic curves (AUCs) for detecting HMG were compared among the instruments and between the two normal groups (HMN or NHMN).

Results. Highly myopic normal eyes showed higher AUCs for the temporal quadrant cpRNFL thickness but lower AUCs for the superior and inferior RNFL thicknesses compared with NHMN. We found the AUCs for the GCC thickness showed no significant difference between the two control groups, but the GCL/IPL and mRNFL thicknesses had differences.

Conclusions. The abilities of the three OCT instruments to detect early glaucomatous eyes with high myopia were different if the normal eyes were associated with high myopia or not. A normative database that includes data from patients with high myopia should be established for accurate diagnosis of glaucoma with high myopia. (www.umin.ac.jp/ctr number, UMIN000006900.)

Keywords: myopia, optical coherence tomography, glaucoma

Myopia is a common ocular abnormality worldwide, and it is an independent risk factor for primary open-angle glaucoma.[1] Although diagnosing glaucoma in myopic subjects is important in clinical practice, structural changes related to myopia such as tilting, optic disc deformation, shallow cup, and large peripapillary crescent hinder the precise diagnosis of glaucoma.[2,3]

Although spectral-domain optical coherence tomography (SD-OCT) has been shown to be useful for identifying glaucomatous damage, a significant proportion of normal myopic eyes is classified as abnormal because the normative database of SD-OCT instruments largely comprise data collected from normal eyes with no or low myopia. Several studies have demonstrated that myopic eyes have thinner circumpapillary retinal nerve fiber layers (cpRNFLs) and a unique pattern of RNFL distribution, leading to inaccurate diagnosis of glaucoma by OCT.[4–10] Our previous study showed that the diagnostic performances of the measurements of the cpRNFL and ganglion cell complex (GCC) thicknesses for the identification of highly myopic glaucoma (HMG) including all stages of visual field (VF) loss from highly myopic controls were relatively high, and similar results were obtained from three different SD-OCTs.[11] Although diagnosing glaucoma with moderate or advanced VF loss is usually not difficult even in highly myopic eyes, it is sometimes difficult to diagnose early glaucoma in highly myopic eyes in the clinical setting. Therefore, it would be valuable if early glaucoma in highly myopic eyes could be distinguished from nonglaucoma using OCT. Furthermore, given that the normative databases of SD-OCT instruments are created from controls without high myopia, misdiagnosis of glaucoma in patients with high myopia may occur when the internal database is used.[12] The present study evaluates the diagnostic performances of different SD-OCTs in their ability to distinguish between HMG and two types of controls, namely highly myopic normal (HMN) eyes or nonhighly myopic normal (NHMN) eyes.

Materials and Methods

All subjects were recruited at the Kobe University Hospital (Kobe, Japan) for this observational cross-sectional study. The institutional review board of Kobe University approved the study protocol, which adhered to the tenets of the Declaration of Helsinki. Written informed consent was obtained from each

subject after an explanation of the study protocol was provided.

All subjects received a full ocular examination. We used a SITA standard program (Humphrey Field Analyzer [HFA] 30-2; Carl Zeiss Meditec, Inc., Dublin, CA, USA) was used to perform the VF test. Subjects with a best-corrected visual acuity of 20/40 or better, a cylinder component of refraction less than 3.0 D, and gonioscopically open angles were included. The subjects were divided into a highly myopic group whose spherical equivalent were less than –6.00 D and a nonhighly myopic group. Axial length was acquired using an optical biometer (IOLMaster; Carl Zeiss Meditec, Inc.). No subjects had undergone any ocular surgeries. The visual field tests, the cpRNFL thickness, and macular parameters were measured using three SD-OCT instruments within 3 months. A total of 52 HMG eyes from 42 subjects and 54 HMN eyes from 36 subjects were enrolled. Additionally, we included 90 NHMN eyes from 67 subjects.

Two independent masked glaucomatous specialists (AA, AK) evaluated the appearance of the stereophotograph of the optic disc obtained by a retinal camera (nonmyd WX3D; Kowa Company, Nagoya, Japan). In case of disagreement, a third specialist (MN) made the final decision. Glaucomatous optic neuropathy (GON) was defined as vertical cup–disc asymmetry between fellow eyes of 0.2 or more with neuroretinal rim damage, such as excavation, rim thinning, and notches with or without peripapillary hemorrhages, or RNFL defects with a reproducible VF defect. The diagnosis of glaucomatous VF defects was based on the following criteria: two or more contiguous points with a pattern deviation sensitivity loss of $P < 0.01$, three or more contiguous points with a sensitivity loss of $P < 0.05$ in the superior or inferior arcuate areas, or a 10 dB difference across the nasal horizontal midline at two or more adjacent locations and an abnormal result on the glaucoma hemifield test.[13] Glaucomatous eyes with early visual field loss (mean deviation > –6.0 dB) were enrolled. Healthy subjects aged at least 20 years were included as controls in the study. The inclusion criteria for normal eyes were as follows: intraocular pressure <21 mm Hg, reliable HFA results (fixation loss, false positive, or false negative >33%), no abnormal HFA findings suggestive of glaucoma (as mentioned above), no retinal diseases, and no GON.

cpRNFL Measurements

The optic disc cube protocol was adopted for the Cirrus HD-OCT (software version 6.1.0.96; Carl Zeiss Meditec, Inc.). This protocol is based on a three-dimensional (3D) scan of a 6- × 6-mm² area that is centered on the optic disc. A 3.46-mm diameter circular scan was performed automatically around the optic disc, which provided measurements of the parapapillary RNFL thickness. Images with signal strengths of <6 were excluded. Thickness values of RNFL at 256 measurement points on the circular scan were exported and evaluated as described below.

The optic nerve head map protocol was applied for RTVue-100 (software version 4.0.5.39; Optovue, Inc., Fremont, CA, USA). This protocol generated an RNFL thickness map that was measured around a circle 3.45 mm in diameter and centered on the optic disc. A 3D disc protocol was used to register the edge of the optic nerve head. Only good quality images, as defined by a signal strength index of >30, were included. Thickness parameters of RNFL were calculated by the built-in software.

The Topcon 3D OCT-2000 (software version 8.00; Topcon, Inc., Tokyo, Japan) uses a 7 × 7 mm scan disc protocol. The magnification effect in each eye was corrected according to the formula (modified Littman's method) provided by the manufacturer, which was based on the refraction, corneal radius, and axial length to obtain more accurate circle sizes during the measurement. Images with a quality factor of >60 were included in the analyses. Thickness data of RNFL with 1024 points of resolution with a 3.46-mm circle diameter were exported by the software from Topcon, Inc., and evaluated as described below.

The thicknesses of RNFL at 256 points from Cirrus, 2325 points from RTVue, and 1024 points from Topcon 3D OCT were converted to the following parameters. The mean 360° RNFL thickness was defined as the mean of the RNFL thicknesses. Starting from a point on the temporal margin, which was designated as 0°, the mean quadrant RNFL thickness between 315° and 45°, 45° and 135°, 135° and 225°, and 225° and 315° were defined as the temporal, superior, nasal, and inferior RNFL thicknesses, respectively.

Macular Inner Retinal Layer Thickness Measurements

Ganglion cell analysis (GCA) was used to process the data produced by Cirrus OCT. Ganglion cell analysis measures the thicknesses of the macular RNFL (mRNFL), ganglion cell layer + inner plexiform layer (GCL/IPL), and mRNFL + GCL/IPL (GCC) within a 14.13-mm² elliptical annulus area centered on the fovea. The special software provided by Zeiss was used to export the data. The superior (0–180°) and inferior (180–360°) segments were calculated from the corresponding sectors.

The ganglion cell complex was measured using the RTVue-100 OCT. The ganglion cell complex protocol explores parameters within a circle 6-mm in diameter; the center of the GCC scan was shifted approximately 1 mm temporal to the fovea to improve the sampling of the temporal peripheral nerve fibers. The variables generated by the GCC analysis included the mean, superior, and inferior hemiretinas.

Raster scanning of a 7-mm² area that was centered on the fovea with a scan density of 512 (vertical) × 128 (horizontal) scans was performed using Topcon 3D OCT-2000. The built-in protocol measured a 6- × 6-mm area that was centered in the fovea using embedded Topcon 3D OCT measurement software. The data were divided into 10 × 10 grids and exported by the software from Topcon, Inc. The mean thickness and superior and inferior hemiretina thicknesses of the mRNFL, GCL/IPL, and GCC were calculated.

Table 1 summarizes the measurement protocols for each instrument.

Statistical Analysis

All numerical data were normally distributed as confirmed by the Kolmogorov-Smirnov test. Bilateral eyes were included in the analyses if they matched the inclusion criteria. As measurements from both eyes of the same subject are likely to be correlated, the standard statistical method for parameter estimation could have led to underestimation of the standard errors (SEs).[14] To compare the thickness for each parameter between the groups, the thickness was adjusted by the correlation between each thickness and age in the NHMN eyes. A generalized linear model was used to evaluate the mean difference between the groups. This method of compensating for age imbalance has been used in a previous ophthalmological study.[15] Measurement parameters of OCT of the different groups were compared using generalized estimating equation models to account for intereye dependencies.

Receiver operating characteristic (ROC) curves were constructed for the cpRNFL, GCC, GCL/IPL, and mRNFL thicknesses to investigate the ability of the devices to differentiate between glaucomatous eyes with high myopia

Table 1. Characteristics of the Studied Eyes (Means ± SD)

	HMN, $n = 54$	NHMN, $n = 90$	HMG, $n = 52$	HMN vs. HMG	NHMN vs. HMG	HMN vs. NHMN
Age, y	39.0 ± 12.4	43.9 ± 13.6	47.9 ± 13.6	0.004*	0.445*	0.128*
(Range)	(22 to 65)	(19 to 68)	(22 to 64)			
Sex, % female	74.1	65.2	55.8	0.066†	0.134†	0.270†
Refraction, D (spherical equivalent)	−7.76 ± 1.85	−2.31 ± 2.1	−7.74 ± 1.55	1.000*	<0.001*	<0.001*
(Range)	(−6.25 to −13.0)	(2.25 to −5.75)	(−6.00 to −13.0)			
Axial length, mm	26.6 ± 0.79	24.8 ± 1.13	26.8 ± 0.85	0.508*	<0.001*	<0.001*
(Range)	(25.8 to 28.8)	(22.72 to 27.54)	(24.39 to 29.00)			
Mean deviation, dB	−0.68 ± 1.22	0.38 ± 3.47	−2.73 ± 1.66	<0.001	<0.001*	0.038*
(Range)	(0.64 to −3.11)	(2.66 to −4.76)	(0.14 to −6.00)			

* Generalized estimating equation model.
† Fisher's exact test.

and HMN eyes or NHMN eyes. To account for potential correlations between the eyes, the data cluster for each subject was considered as the unit of resampling when calculating SEs. This procedure has previously been used in the literature to adjust for the presence of multiple correlated measurements from the same unit.[16] The curves of ROC were adjusted for differences in age and sex using covariate-adjusted ROC curves, as established by Pepe.[17] A bootstrap resampling procedure was used ($n = 1000$ resamples). The area under the ROC curve was calculated for each parameter, and a pairwise comparison of the AUCs was performed using the method proposed by Dodd and Pepe.[18] When the estimated correlation between the two instruments was set at 0.8, a minimum of 36 cases in the positive and negative groups were required to detect a 0.1 difference in the AUCs at values of more than 0.8. These findings were achieved at a statistical power of 80% and a type I error of 5%. To compare AUCs between the controls with or without high myopia to detect HMG eyes, a bootstrapping procedure was performed to obtain 95% confidence intervals (CIs) using 2.5% and 97.5% of each AUC from the bootstrapped distribution. The area under the ROC curve were then compared by *t*-tests to test the null hypothesis that the means of the AUCs are equivalent in the two models.

Statistical analyses were performed using statistical software (ver. 12.0; StataCorp., College Station, TX, USA, and SPSS, ver. 20.0; Japan IBM, Tokyo, Japan) and the open programming language R (ver. 2.13.2, http://www.r-project.org; R Foundation for Statistical Computing, Vienna, Austria). Values of $P < 0.05$ were considered statistically significant.

Results

Table 1 presents the demographics and ocular characteristics of the subjects. No significant differences were found in terms of the refraction and axial length between the normal and glaucomatous eyes with high myopia. However, there were

Table 2. Circumpapillary RNFL Thickness Measured by SD-OCT Instruments Adjusted by Age (Mean ± SD)

				P Value		
cpRNFL thickness, µm	HMN, $n = 54$	NHMN, $n = 90$	HMG, $n = 52$	HMN vs. HMG	NHMN vs. HMG	HMN vs. NHMN
Cirrus						
Average	89.8 ± 7.9	93.5 ± 6.9	69.4 ± 11.3	<0.001*	<0.001*	0.034*
Superior	107.4 ± 15.8	115.0 ± 13.2	83.8 ± 16.6	<0.001*	<0.001*	0.024*
Nasal	64.2 ± 9.9	66.8 ± 9.0	66.4 ± 16.6	1.000	1.000	0.558
Inferior	102.7 ± 15.9	118.0 ± 12.4	72.5 ± 17.7	<0.001*	<0.001*	<0.001*
Temporal	85.2 ± 17.0	74.1 ± 11.2	66.7 ± 14.5	<0.001*	0.029*	0.001*
RTVue						
Superior	110.4 ± 14.4	123.8 ± 14.3	95.9 ± 17.3	<0.001*	<0.001*	<0.001*
Nasal	65.6 ± 16.3	69.9 ± 10.0	57.8 ± 9.2	0.005*	<0.001*	0.311
Inferior	121.6 ± 14.9	132.2 ± 13.5	89.6 ± 16.6	<0.001*	<0.001*	<0.001*
Temporal	87.8 ± 13.2	83.0 ± 10.6	72.9 ± 16.3	<0.001*	0.002*	0.075
3D OCT						
Average	99.0 ± 10.2	103.2 ± 7.9	77.1 ± 11.8	<0.001*	<0.001*	0.059
Superior	117.9 ± 17.8	127.1 ± 14.1	95.9 ± 19.7	<0.001*	<0.001*	0.008*
Nasal	65.0 ± 14.7	76.0 ± 14.5	62.0 ± 10.0	0.825	<0.001*	<0.001*
Inferior	123.5 ± 17.3	130.4 ± 13.6	84.9 ± 20.8	<0.001*	<0.001*	0.086
Temporal	91.9 ± 16.8	81.3 ± 12.2	74.9 ± 21.5	<0.001*	0.231	0.002*

* $P < 0.05$

Table 3. Inner Retinal Layer Parameters by SD-OCT Instruments Adjusted by Age (Mean ± SD)

Macular Thickness, μm	HMN, $n = 54$	NHMN, $n = 90$	HMG, $n = 52$	*P* Value: HMN vs. HMG	*P* Value: NHMN vs. HMG	*P* Value: HMN vs. NHMN
Cirrus						
GCC						
Average	110.9 ± 10.5	115.9 ± 7.4	97.3 ± 11.9	<0.001*	<0.001*	0.012*
Superior	111.5 ± 10.4	115.3 ± 7.6	101.6 ± 12.2	<0.001*	<0.001*	0.088
Inferior	110.5 ± 11.0	116.3 ± 7.7	93.2 ± 14.2	<0.001*	<0.001*	0.003*
GCL/IPL						
Average	75.8 ± 6.7	81.5 ± 6.6	67.0 ± 7.0	<0.001*	<0.001*	<0.001*
Superior	76.7 ± 6.9	82.1 ± 5.9	69.6 ± 7.4	<0.001*	<0.001*	<0.001*
Inferior	75.0 ± 6.9	81.4 ± 6.0	64.3 ± 7.9	<0.001*	<0.001*	<0.001*
mRNFL						
Average	35.2 ± 4.4	34.0 ± 3.0	30.6 ± 5.5	<0.001*	0.001*	0.217
Superior	35.0 ± 4.3	33.2 ± 3.5	32.0 ± 5.8	0.017*	0.689	0.040*
Inferior	35.6 ± 4.9	34.8 ± 3.2	28.8 ± 7.1	<0.001*	<0.001*	0.911
RTVue						
GCC						
Average	89.1 ± 5.1	93.9 ± 6.7	79.6 ± 9.9	<0.001*	<0.001*	<0.001*
Superior	89.8 ± 5.2	93.7 ± 7.3	80.2 ± 9.6	<0.001*	<0.001*	0.002*
Inferior	89.3 ± 6.2	94.1 ± 6.7	72.4 ± 14.2	<0.001*	<0.001*	0.001*
3D OCT						
GCC						
Average	103.0 ± 5.5	105.0 ± 7.2	87.5 ± 10.3	<0.001*	<0.001*	0.256
Superior	103.0 ± 5.5	104.1 ± 7.4	92.4 ± 10.8	<0.001*	<0.001*	1.000
Inferior	103.0 ± 6.4	105.9 ± 7.6	75.1 ± 13.0	<0.001*	<0.001*	0.054
GCL/IPL						
Average	68.2 ± 3.7	70.0 ± 5.1	60.7 ± 6.1	<0.001*	<0.001*	0.101
Superior	69.4 ± 3.8	70.8 ± 5.2	63.5 ± 6.5	<0.001*	<0.001*	0.269
Inferior	67.1 ± 3.9	69.1 ± 5.3	57.9 ± 6.7	<0.001*	<0.001*	0.047*
mRNFL						
Average	34.8 ± 3.1	35.0 ± 3.6	26.9 ± 5.1	<0.001*	<0.001*	1.000
Superior	33.6 ± 3	33.2 ± 3.7	28.9 ± 5.6	<0.001*	<0.001*	1.000
Inferior	35.9 ± 4	36.8 ± 4.3	24.8 ± 6.6	<0.001*	<0.001*	0.750

* $P < 0.05$

significant differences in age; hence, the AUCs were adjusted for these covariates.

Table 2 summarizes the cpRNFL thicknesses in the three groups. Except for the nasal quadrant, the cpRNFL thickness parameters were significantly thinner in the HMG eyes than in the HMN and NHMN eyes. In the nasal quadrant, only RTVue was found to be thinner in the HMG eyes than in the HMN and NHMN eyes; however, this was not detected by Cirrus or Topcon 3D OCT. The mean cpRNFL thicknesses as detected by all three instruments were thinner in the HMN eyes than in the NHMN eyes. For the superior and inferior quadrants, the cpRNFL thicknesses were thinner in the HMN eyes than in the NHMN eyes for all instruments. The thicknesses of the temporal quadrant in the HMN eyes were more than those in the NHMN eyes for Cirrus and 3D OCT, although this difference was not statistically significant for RTVue.

Table 3 summarizes the mean thicknesses of the macular parameters in the three groups. All of the parameters in the HMG eyes were significantly thinner than those in both the HMN and NHMN eyes. There were no significant differences in the mean GCC thickness between the two control groups for Cirrus or Topcon 3D OCT; in contrast, the mean GCC was thinner in the HMN eyes than in the NHMN eyes for RTVue. The mean GCL/IPL was thinner in HMN eyes than in NHMN eyes for Cirrus and Topcon 3D OCT. The mean mRNFL for Cirrus was thicker in the HMN eyes than in the NHMN eyes. There were no significant differences in the mean mRNFL thickness between the two normal groups as shown by Topcon 3D OCT.

Table 4 shows the AUCs of the parameters for each instrument to distinguish the HMG eyes from the HMN eyes. The values of AUC for the mean cpRNFL thickness were 0.942, 0.953, and 0.933 for Cirrus, RTVue, and Topcon 3D OCT, respectively. Among the instruments, no significant differences were observed in the cpRNFL thickness of the mean and four quadrants other than the nasal quadrant ($P < 0.05$). RTVue exhibited a significantly higher AUC for the nasal quadrant compared with Cirrus ($P = 0.0035$) and Topcon 3D OCT ($P = 0.0054$). Regarding the macular parameters, the AUCs for the mean GCC were 0.899, 0.919, and 0.940 for Cirrus, RTVue, and Topcon 3D OCT, respectively. There were no significant differences in the mean and two-hemifield GCC thicknesses among the instruments. RTVue is not able to discriminate between GCL/IPL and mRNFL; therefore, the segmented parameters were only compared between Cirrus and Topcon 3D OCT. No significant differences in the AUCs of the mean

Table 4. Area Under the ROC Curve Analysis for Diagnosing HMG Eyes (Means ± SE) From Normal Eyes With or Without High Myopia

	SD-OCT Instruments			SD-OCT Instruments			*P* Value		
	NHMN			HMN			NHMN vs. HMN		
Measured Thickness Parameters	**Cirrus**	**RTVue**	**3D OCT**	**Cirrus**	**RTVue**	**3D OCT**	**Cirrus**	**RTVue**	**3D OCT**
CpRNFL									
Average	0.975 (±0.015)	0.962 (±0.018)	0.972 (±0.015)	0.942 (±0.029)	0.953 (±0.028)	0.933 (±0.033)	0.003	0.380	0.001
Quadrant									
Superior	0.930 (±0.032)	0.899 (±0.035)	0.898 (±0.035)	0.881 (±0.045)	0.805 (±0.055)	0.803 (±0.052)	0.001	<0.001	<0.001
Temporal	0.663 (±0.064)	0.713 (±0.058)	0.674 (±0.063)	0.835 (±0.056)	0.821 (±0.050)	0.812 (±0.056)	<0.001	<0.001	<0.001
Inferior	0.976 (±0.014)	0.957 (±0.025)	0.961 (±0.020)	0.923 (±0.034)	0.917 (±0.036)	0.942 (±0.031)	<0.001	0.008	0.131
Nasal	0.572 (±0.070)	0.839 (±0.038)	0.781 (±0.043)	0.566 (±0.072)	0.751 (±0.056)	0.579 (±0.071)	0.887	<0.001	<0.001
GCC									
Average	0.910 (±0.032)	0.939 (±0.038)	0.930 (±0.026)	0.889 (±0.052)	0.919 (±0.039)	0.94 (±0.024)	0.312	0.297	0.425
Superior	0.839 (±0.047)	0.884 (±0.044)	0.820 (±0.045)	0.823 (±0.070)	0.878 (±0.054)	0.857 (±0.057)	0.580	0.808	0.141
Inferior	0.929 (±0.028)	0.946 (±0.034)	0.944 (±0.022)	0.887 (±0.048)	0.913 (±0.036)	0.938 (±0.029)	0.025	0.058	0.633
GCL/IPL									
Average	0.947 (±0.025)	NA NA	0.896 (±0.037)	0.9 (±0.056)	NA NA	0.891 (±0.061)	0.022		0.837
Superior	0.920 (±0.035)	NA NA	0.817 (±0.051)	0.844 (±0.075)	NA NA	0.812 (±0.084)	0.006		0.881
Inferior	0.961 (±0.023)	NA NA	0.918 (±0.031)	0.908 (±0.049)	NA NA	0.9 (±0.045)	0.004		0.337
mRNFL		NA			NA				
Average	0.741 (±0.056)	NA NA	0.911 (±0.031)	0.863 (±0.047)	NA NA	0.94 (±0.027)	<0.001		0.005
Superior	0.589 (±0.063)	NA NA	0.760 (±0.051)	0.795 (±0.054)	NA NA	0.865 (±0.049)	<0.001		<0.001
Inferior	0.785 (±0.054)	NA NA	0.929 (±0.027)	0.836 (±0.052)	NA NA	0.939 (±0.027)	0.054		0.457

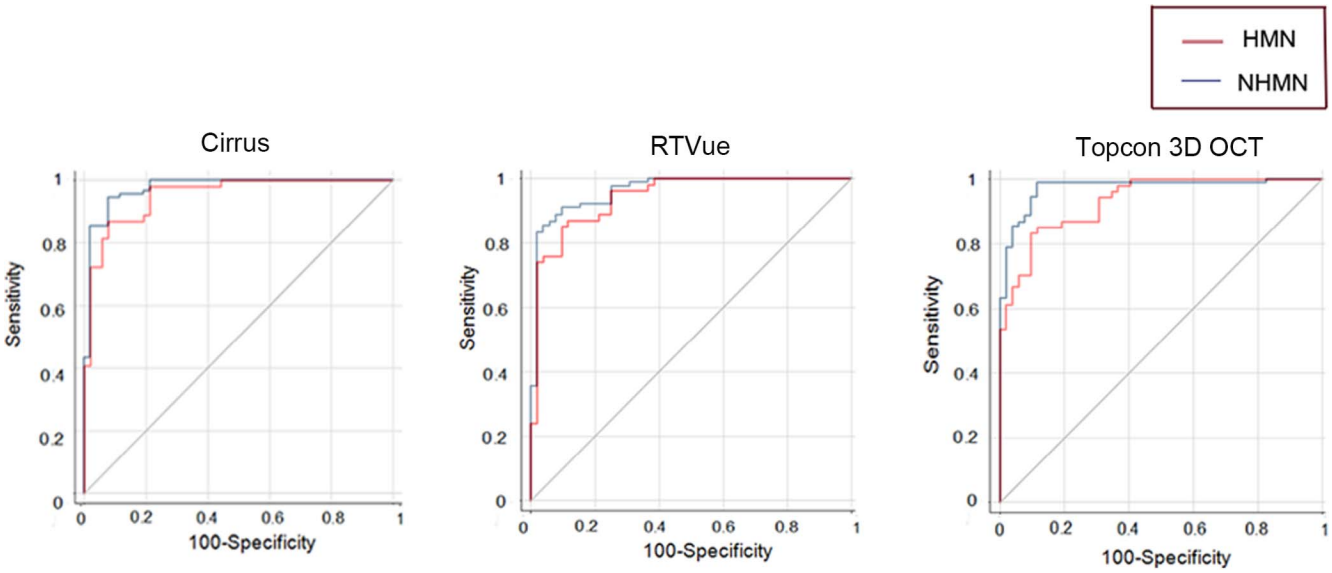

Figure 1. Receiver operating characteristic curves of the mean cpRNFL thickness using Cirrus, RTVue, and Topcon 3D OCT for discriminating highly myopic glaucomatous eyes from HMN or NHMN eyes.

Investigative Ophthalmology & Visual Science

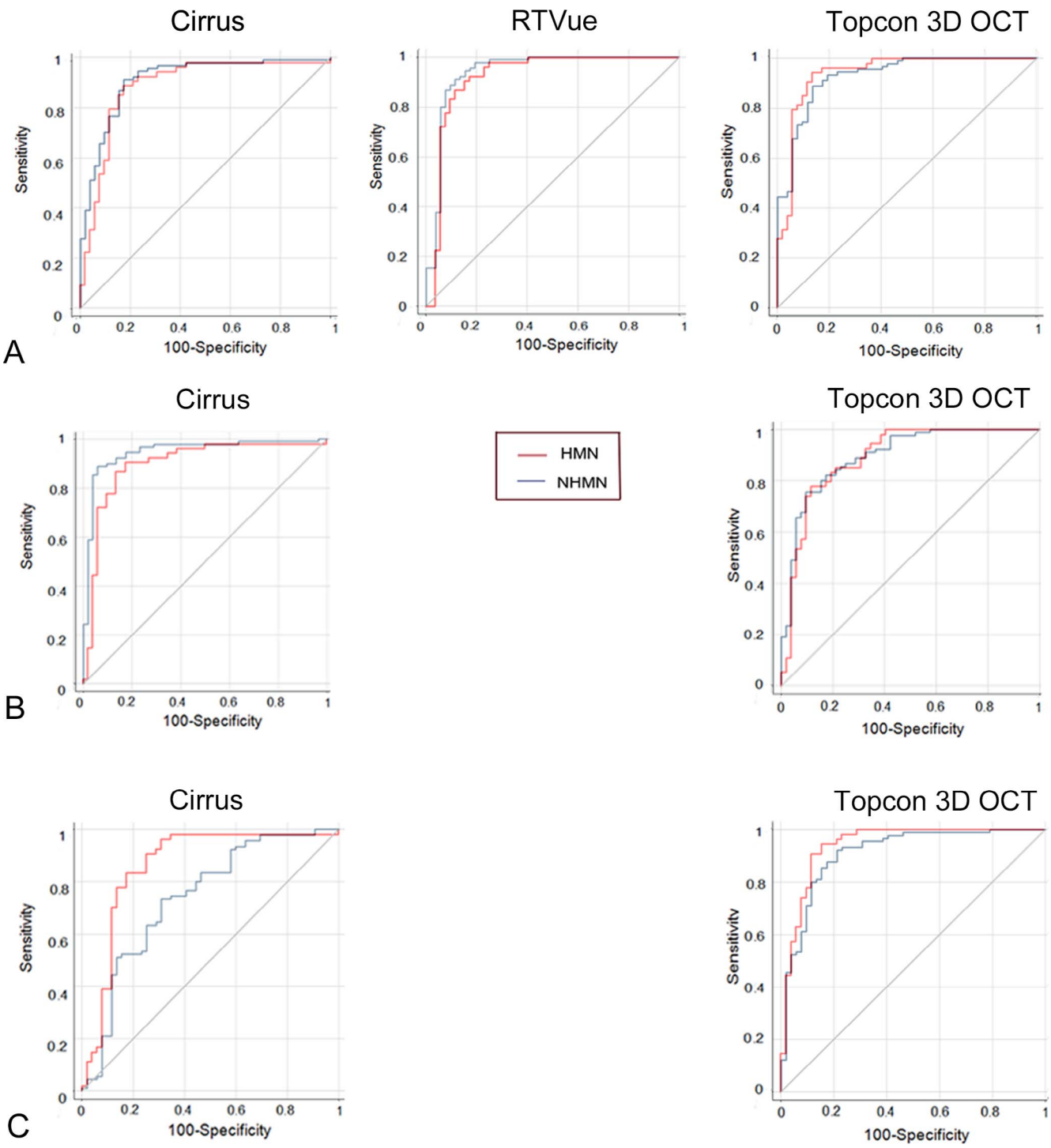

FIGURE 2. Receiver operating characteristic curves of the mean GCC thickness (**A**), the mean GCL/IPL thickness (**B**), and the mean mRNFL thickness (**C**) measured using Cirrus, RTVue, and Topcon 3D OCT for discriminating highly myopic glaucomatous eyes from HMN or NHMN eyes.

and two-hemifield GCL/IPL thicknesses were observed among the instruments. Topcon 3D OCT exhibited significantly higher AUCs for the mean and inferior-hemifield mRNFL measurements compared with Cirrus.

Table 4 also compares the AUCs for the detection of the early HMG eyes from the NHMN and HMN eyes for each instrument. Figure 1 illustrates the ROC curves of cpRNFL for distinguishing the HMG eyes from the NHMN eyes. Compared with the NHMN controls, the AUCs in the temporal quadrant for the cpRNFL thickness were higher for all three instruments, but lower in the superior, inferior, and nasal quadrants compared with the HMN. Figure 2 shows the ROC curves of macular parameters for distinguishing the HMG eyes from the NHMN eyes. There were no significant differences in the mean and two-hemifield GCC thicknesses for all instruments between the two controls. The values of AUC for the mean and two-hemifield GCL/IPL thicknesses were lower in the HMN eyes than in the NHMN eyes for Cirrus. In addition, the

AUC of the mean and superior-hemifield mRNFL thicknesses in the HMN eyes were higher than those in the NHMN eyes for the two instruments.

Discussion

First, we need to consider the differences in the thicknesses as measured by OCT between the normal and myopic eyes. Previous studies have shown that compared with emmetropic eyes, myopic eyes have thinner mean cpRNFL measurements in OCT.[4–7] Myopia has also been shown to affect the distribution pattern of the RNFL thickness around the optic disc; with increasing myopia, the superotemporal and inferotemporal RNFL bundles tend to converge temporally.[8–10] In this study, the mean and inferior and superior quadrant cpRNFL thicknesses were thinner in the HMN eyes than in the NHMN eyes. Contrarily, the temporal cpRNFL thickness in the HMN eyes was thicker. These findings are in agreement with those from previous studies.[7,19,20]

We also evaluated the difference in the ability of the AUCs to distinguish between early HMG and normal eyes with or without high myopia. When the normal eyes were set as the HMN eyes, lower AUCs in the mean, superior, inferior, and nasal quadrant cpRNFL thicknesses, except for the mean cpRNFL for RTVue, the inferior quadrant for Topcon 3D OCT, and the nasal quadrant for Cirrus were found compared with the NHMN eyes. For the average cpRNFL, longer axial length lead to scan larger area. As a result of this magnification effect, the measured average cpRNFL thickness become thinner to distant to optic disc. Thus values of AUC for average cpRNFL were better in nonhighly myopic normal eyes than highly myopic normal eyes. Contrasting results were observed for the temporal quadrant in all instruments. As the normative data of recent SD-OCTs are based on NHMN eyes, our results indicate that the use of cpRNFL thicknesses (except for the temporal quadrant) to detect HMG may lead to false positive diagnosis when the internal database is used. Conversely, the opposite is true for the temporal quadrant cpRNFL thickness. Yamashita et al.[10] demonstrated that longer axial length is significantly associated with increased rates of supernormal thickness in the temporal area, as well as higher rates of false positives and abnormal thinning with redness in the superior and inferior sectors. These observations are consistent with our results. Therefore, it is important to be aware that using the internal database may lead to inappropriate interpretation of cpRNFL thicknesses when evaluating glaucoma with high myopia. Thus, a normal database from normal eyes with high myopia should be installed as internal data in OCT instruments.

Previous studies have obtained conflicting results on the effect of myopia on macular parameters. Some studies found a correlation between total macular thickness and axial length,[21,22] whereas others did not.[23,24] Likewise, some previous studies, including ours, showed a negative correlation between axial length and macular inner retinal layer thicknesses,[25,26] whereas another study did not.[27] In this study, there were no significant differences in the mean GCC thickness between the HMN and NHMN eyes for Cirrus and Topcon 3D OCT, and the mean GCL/IPL thicknesses were thinner in the HMN eyes than in the NHMN eyes for Cirrus and Topcon 3D OCT. Previous studies reported that abnormal GCA diagnostic classification was associated with longer axial length.[28,29] This study also showed that the AUCs for the mean GCL/IPL thickness were lower in the HMN eyes than in the NHMN eyes, which could be due to the following two reasons: retinal thinning associated with the extension of the retinal surface due to axial elongation[4] or the projection artifact of the scanning area of the OCT instruments in HMN eyes. As a larger area is scanned in eyes with longer axis length, the measured thickness may change. The ganglion cell layer/IPL is the thickest in the parafoveal area and becomes thinner to distant to parafovea.[27] This suggests that a wider scanning area results in thinner GCL/IPL values.[26] On the contrary, the mRNFL is thin at the central fovea and becomes thicker to distant fovea. When the scanning area widens, the mRNFL appears to thicken. Essentially, the mRNFL was thicker in the HMN eyes than in the NHMN eyes for Cirrus. The thickness of mRNFL had lower AUCs in the HMN eyes than in the NHMN eyes for both Cirrus and Topcon 3D OCT. In summary, to detect HMG, the current internal database using NHMN eyes tends to results in false diagnosis in terms of the GCL/IPL thickness and mRNFL thickness.

Our study has some limitations. First, the HFA and OCT measurements were not performed on the same day in most subjects. However, these examinations were performed within 3 months. All glaucomatous eyes exhibited stable intraocular pressure, and the treatment modality was not altered during the study. Therefore, changes in the examined parameters during the examination period were likely negligible. Second, our study's design was a case-control study including patients with well-established glaucoma, and the separate group of normal subjects used as hospital-based controls could have resulted in substantially overestimated diagnostic performance.[30,31]

In conclusion, significant differences were observed in the diagnostic performances of the cpRNFL thickness measurements between the HMN and NHMN groups to detect highly myopic glaucoma with early VF loss using three different types of SD-OCTs. As for the GCC thickness, the difference was not statistically significant. However, the mRNFL lead to false positive high detection for glaucoma with high myopia. Although the usage of SD-OCT in glaucoma is not commercially recommended in highly myopic eyes, these instruments would be more precise for diagnosing HMG if a normative database in highly myopic eyes was available.

Acknowledgments

Presented at the annual meeting of the Association for Research in Vision and Ophthalmology, Denver, Colorado, United States, May 2015.

Supported by JSPS KAKENHI Grant Number 25462715 (AK) from the Japanese Government, the Mishima Memorial Foundation (AK), and the Santen Pharmaceutical Founder Commemoration Ophthalmic Research Fund (AK).

Disclosure: **A. Akashi**, None; **A. Kanamori**, None; **K. Ueda**, None; **Y. Inoue**, None; **Y. Yamada**, None; **M. Nakamura**, None

References

1. Mitchell P, Hourihan F, Sandbach J, Wang JJ. The relationship between glaucoma and myopia: the Blue Mountains Eye Study. *Ophthalmology*. 1999;106:2010–2015.
2. Xu L, Wang Y, Wang S, Wang Y, Jonas JB. High myopia and glaucoma susceptibility the Beijing Eye Study. *Ophthalmology*. 2007;114:216–220.
3. Witmer MT, Margo CE, Drucker M. Tilted optic disks. *Surv Ophthalmol*. 2010;55:403–428.
4. Leung CK, Mohamed S, Leung KS, et al. Retinal nerve fiber layer measurements in myopia: an optical coherence tomography study. *Invest Ophthalmol Vis Sci*. 2006;47:5171–5176.
5. Nagai-Kusuhara A, Nakamura M, Fujioka M, Tatsumi Y, Negi A. Association of retinal nerve fibre layer thickness measured by confocal scanning laser ophthalmoscopy and optical coherence tomography with disc size and axial length. *Br J Ophthalmol*. 2008;92:186–190.

6. Vernon SA, Rotchford AP, Negi A, Ryatt S, Tattersal C. Peripapillary retinal nerve fibre layer thickness in highly myopic Caucasians as measured by Stratus optical coherence tomography. *Br J Ophthalmol*. 2008;92:1076–1080.
7. Kang SH, Hong SW, Im SK, Lee SH, Ahn MD. Effect of myopia on the thickness of the retinal nerve fiber layer measured by Cirrus HD optical coherence tomography. *Invest Ophthalmol Vis Sci*. 2010;51:4075–4083.
8. Kim MJ, Lee EJ, Kim TW. Peripapillary retinal nerve fibre layer thickness profile in subjects with myopia measured using the Stratus optical coherence tomography. *Br J Ophthalmol*. 2010; 94:115–120.
9. Leung CK, Yu M, Weinreb RN, et al. Retinal nerve fiber layer imaging with spectral-domain optical coherence tomography: interpreting the RNFL maps in healthy myopic eyes. *Invest Ophthalmol Vis Sci*. 2012;53:7194–7200.
10. Yamashita T, Asaoka R, Tanaka M, et al. Relationship between position of peak retinal nerve fiber layer thickness and retinal arteries on sectoral retinal nerve fiber layer thickness. *Invest Ophthalmol Vis Sci*. 2013;54:5481–5488.
11. Akashi A, Kanamori A, Nakamura M, Fujihara M, Yamada Y, Negi A. The ability of macular parameters and circumpapillary retinal nerve fiber layer by three SD-OCT instruments to diagnose highly myopic glaucoma. *Invest Ophthalmol Vis Sci*. 2013;54:6025–6032.
12. Yamashita T, Kii Y, Tanaka M, et al. Relationship between supernormal sectors of retinal nerve fibre layer and axial length in normal eyes. *Acta Ophthalmol*. 2014;92:e481–e487.
13. Anderson DR, Patella VM. *Automated Static Perimetry*. 2nd ed. St. Louis: Mosby; 1999.
14. Glynn RJ, Rosner B. Accounting for the correlation between fellow eyes in regression analysis. *Arch Ophthalmol*. 1992; 110:381–387.
15. Tan O, Chopra V, Lu AT, et al. Detection of macular ganglion cell loss in glaucoma by Fourier-domain optical coherence tomography. *Ophthalmology*. 2009;116:2305–2314.e1-e2.
16. Alonzo TA, Pepe MS. Distribution-free ROC analysis using binary regression techniques. *Biostatistics*. 2002;3:421–432.
17. Pepe MS. *The Statistical Evaluation of Medical tests for Classification and Prediction*. Oxford: Oxford University Press; 2004:xvi, 302.
18. Dodd LE, Pepe MS. Partial AUC estimation and regression. *Biometrics*. 2003;59:614–623.
19. Choi YJ, Jeoung JW, Park KH, Kim DM. Glaucoma detection ability of ganglion cell-inner plexiform layer thickness by spectral-domain optical coherence tomography in high myopia. *Invest Ophthalmol Vis Sci*. 2013;54:2296–2304.
20. Kim NR, Lee ES, Seong GJ, et al. Comparing the ganglion cell complex and retinal nerve fibre layer measurements by Fourier domain OCT to detect glaucoma in high myopia. *Br J Ophthalmol*. 2011;95:1115–1121.
21. Lam DS, Leung KS, Mohamed S, et al. Regional variations in the relationship between macular thickness measurements and myopia. *Invest Ophthalmol Vis Sci*. 2007;48:376–382.
22. Song WK, Lee SC, Lee ES, Kim CY, Kim SS. Macular thickness variations with sex, age, and axial length in healthy subjects: a spectral domain-optical coherence tomography study. *Invest Ophthalmol Vis Sci*. 2010;51:3913–3918.
23. Chan CM, Yu JH, Chen LJ, et al. Posterior pole retinal thickness measurements by the retinal thickness analyzer in healthy Chinese subjects. *Retina*. 2006;26:176–181.
24. Zou H, Zhang X, Xu X, Yu S. Quantitative in vivo retinal thickness measurement in Chinese healthy subjects with retinal thickness analyzer. *Invest Ophthalmol Vis Sci*. 2006;47: 341–347.
25. Mwanza JC, Durbin MK, Budenz DL, et al. Profile and predictors of normal ganglion cell-inner plexiform layer thickness measured with frequency-domain optical coherence tomography. *Invest Ophthalmol Vis Sci*. 2011;52:7872–7879.
26. Ueda K, Kanamori A, Akashi A, Tomioka M, Kawaka Y, Nakamura M. Effects of axial length and age on circumpapillary retinal nerve fiber layer and inner macular parameters measured by 3 types of SD-OCT instruments [published online ahead of print January 14, 2015]. *J Glaucoma*. doi:10.1097/IJG.0000000000000216.
27. Ooto S, Hangai M, Tomidokoro A, et al. Effects of age, sex, and axial length on the three-dimensional profile of normal macular layer structures. *Invest Ophthalmol Vis Sci*. 2011; 52:8769–8779.
28. Hwang YH, Jeong YC, Kim HK, Sohn YH. Macular ganglion cell analysis for early detection of glaucoma. *Ophthalmology*. 2014;121:1508–1515.
29. Kim KE, Jeoung JW, Park KH, Kim DM, Kim SH. Diagnostic classification of macular ganglion cell and retinal nerve fiber layer analysis: differentiation of false-positives from glaucoma. *Ophthalmology*. 2015;122:502–510.
30. Medeiros FA, Ng D, Zangwill LM, Sample PA, Bowd C, Weinreb RN. The effects of study design and spectrum bias on the evaluation of diagnostic accuracy of confocal scanning laser ophthalmoscopy in glaucoma. *Invest Ophthalmol Vis Sci*. 2007;48:214–222.
31. Rao HL, Kumbar T, Addepalli UK, et al. Effect of spectrum bias on the diagnostic accuracy of spectral-domain optical coherence tomography in glaucoma. *Invest Ophthalmol Vis Sci*. 2012;53:1058–1065.

Investigative Ophthalmology & Visual Science